Comparison of 128-SP-QAM and PM-16QAM in long-haul WDM transmission

Comparison of 128-SP-QAM and PM-16QAM in long-haul WDM transmission

Tobias A. Eriksson,* Martin Sjödin, Pontus Johannisson, Peter A. Andrekson, and Magnus Karlsson

Photonics Laboratory, Department of Microtechnology and Nanoscience, Chalmers University of Technology, SE-412 96, Gothenburg, Sweden

*tobias.eriksson@chalmers.se

Abstract: We investigate 128-level set-partitioning quadrature amplitude modulation (128-SP-QAM) experimentally and compare the performance to polarization-multiplexed 16QAM both at the same bit rate and at the same symbol rate. Using a recirculating loop we study both single channel and wavelength-division multiplexing (WDM) transmission and demonstrate a reach of up to 2680 km at a bit-error rate of 10^{-3} for 128-SP-QAM. We confirm that 128-SP-QAM has an increased sensitivity compared to PM-16QAM and show that the maximum transmission distance can be increased by more than 50 % at the same bit rate for both single channel and WDM transmission. We also investigate the performance at the same symbol rate as a possible fall back solution in a degrading link.

OCIS codes: (060.1660) Coherent communications; (060.4080) Modulation; (060.2360) Fiber optics links and subsystems; (060.2330) Fiber optics communications.

References and links

1. H. Sun, K. Wu, and K. Roberts, "Real-time measurements of a 40 Gb/s coherent system," Opt. Express **16**, 873–879 (2008).
2. T. Pfau, S. Hoffmann, R. Peveling, S. Ibrahim, O. Adamczyk, M. Porrmann, S. Bhandare, R. Noe, and Y. Achiam, "Synchronous QPSK transmission at 1.6 Gbit/s with standard DFB lasers and real-time digital receiver," Electron. Lett. **42**, 1175–1176 (2006).
3. P. J. Winzer, A. H. Gnauck, C. R. Doerr, M. Magarini, and L. L. Buhl, "Spectrally efficient long-haul optical networking using 112-Gb/s polarization-multiplexed 16-QAM," J. Lightwave Technol. **28**, 547–556 (2010).
4. A. Sano, H. Masuda, T. Kobayashi, M. Fujiwara, K. Horikoshi, E. Yoshida, Y. Miyamoto, M. Matsui, M. Mizoguchi, H. Yamazaki, Y. Sakamaki, and H. Ishii, "69.1-Tb/s (432 × 171-Gb/s) C- and extended L-band transmission over 240 Km using PDM-16-QAM modulation and digital coherent detection," in *Optical Fiber Communication Conference/National Fiber Optic Engineers Conference*, (2010), paper PDPB7.
5. H. Bülow, "Polarization QAM modulation (POLQAM) for coherent detection schemes," in *Optical Fiber Communication Conference and National Fiber Optic Engineers Conference*, (2009), paper OWG2.
6. E. Agrell and M. Karlsson, "Power-efficient modulation formats in coherent transmission systems," J. Lightwave Technol. **27**, 5115–5126 (2009).
7. M. Karlsson and E. Agrell, "Which is the most power-efficient modulation format in optical links?" Opt. Express **17**, 10814–10819 (2009).
8. G. Ungerboeck, "Channel coding with multilevel / phase signals," IEEE Trans. Inf. Theory **28**, 55–67 (1982).
9. M. Nölle, J. K. Fischer, L. Molle, C. Schmidt-Langhorst, D. Peckham, and C. Schubert, "Comparison of 8×112 Gb/s PS-QPSK and PDM-QPSK signals over transoceanic distances," Opt. Express **19**, 24370–24375 (2011).
10. M. Sjödin, P. Johannisson, H. Wymeersch, P. A. Andrekson, and M. Karlsson, "Comparison of polarization-switched QPSK and polarization-multiplexed QPSK at 30 Gbit/s," Opt. Express **19**, 7839–7846 (2011).
11. D. Millar, D. Lavery, S. Makovejs, C. Behrens, B. Thomsen, P. Bayvel, and S. Savory, "Generation and long-haul transmission of polarization-switched QPSK at 42.9 Gb/s," Opt. Express **19**, 9296–9302 (2011).

#192613 - $15.00 USD Received 19 Jun 2013; revised 29 Jul 2013; accepted 29 Jul 2013; published 7 Aug 2013

12. J. K. Fischer, S. Alreesh, R. Elschner, F. Frey, C. Meuer, L. Molle, C. Schmidt-Langhorst, T. Tanimura, and C. Schubert, "Experimental Investigation of 126-Gb/s 6PolSK-QPSK Signals," in *European Conference and Exhibition on Optical Communication*, (2012), paper We.1.C.4.
13. H. Bülow, T. Rahman, F. Buchali, W. Idler, and W. Kuebart, "Transmission of 4-D modulation formats at 28-Gbaud," in *Optical Fiber Communication Conference/National Fiber Optic Engineers Conference*, (2013), paper JW2A.39.
14. M. Karlsson and E. Agrell, "Four-dimensional optimized constellations for coherent optical transmission systems," in *European Conference and Exhibition on Optical Communication* (2010), paper We.8.C.3.
15. M. Karlsson and E. Agrell, "Generalized pulse-position modulation for optical power-efficient communication," in *European Conference and Exhibition on Optical Communication*, (2011), paper Tu.6.B.6.
16. X. Liu, T. Wood, R. Tkach, and S. Chandrasekhar, "Demonstration of record sensitivity in an optically pre-amplified receiver by combining PDM-QPSK and 16-PPM with pilot-assisted digital coherent detection," in *Optical Fiber Communication Conference/National Fiber Optic Engineers Conference*, (2011), paper PDPB1.
17. X. Liu, S. Chandrasekhar, T. Wood, R. Tkach, P. Winzer, E. Burrows, and A. Chraplyvy, "M-ary pulse-position modulation and frequency-shift keying with additional polarization/phase modulation for high-sensitivity optical transmission," Opt. Express **19**, B868–B881 (2011).
18. S. Okamoto K. Toyoda, T. Omiya, K. Kasai, M. Yoshida, and M. Nakazawa, "512 QAM (54 Gbit/s) coherent optical transmission over 150 km with an optical bandwidth of 4.1 GHz," in *European Conference and Exhibition on Optical Communication*, (2010), paper PD 2.3.
19. Y. Koizumi, K. Toyoda, M. Yoshida, and M. Nakazawa, "1024 QAM (60 Gbit/s) single-carrier coherent optical transmission over 150 km," Opt. Express **20**, 12508–12514 (2012).
20. L. Coelho and N. Hanik, "Global otimization of fiber-optic communication systems using four-dimensional modulation formats," in *European Conference and Exhibition on Optical Communication*, (2011), paper Mo.2.B.4.
21. M. Karlsson and E. Agrell, "Spectrally efficient four-dimensional modulation," in *Optical Fiber Communication Conference and National Fiber Optic Engineers Conference*, (2012), paper OTu2C.1.
22. J. Renaudier, A. Voicila, O. Bertran-Pardo, O. Rival, M. Karlsson, G. Charlet, and S. Bigo, "Comparison of set-partitioned two-polarization 16QAM formats with PDM-QPSK and PDM-8QAM for optical transmission systems with error-correction coding," in *European Conference and Exhibition on Optical Communication*, (2012), paper We.1.C.5.
23. M. Sjödin, P. Johannisson, J. Li, E. Agrell, P. Andrekson, and M. Karlsson, "Comparison of 128-SP-QAM with PM-16-QAM," Opt. Express **20**, 8356–8366 (2012).
24. H. Zhang, H. G. Batshon, D. G. Foursa, M. Mazurczyk, J.-X. Cai, C. R. Davidson, A. Pilipetskii, G. Mohs, and N. S. Bergano, "30.58 Tb/s transmission over 7,230 km using PDM half 4D-16QAM coded modulation with 6.1 b/s/Hz spectral efficiency," in *Optical Fiber Communication Conference/National Fiber Optic Engineers Conference*, (2013), paper OTu2B.3.
25. H. Zhang, J.-X. Cai, H.G. Batshon, M. Mazurczyk, O.V. Sinkin, D.G. Foursa, A. Pilipetskii, G. Mohs, and N.S. Bergano, "200 Gb/s and dual wavelength 400 Gb/s transmission over transpacific distance at 6 b/s/Hz spectral efficiency," in *Optical Fiber Communication Conference/National Fiber Optic Engineers Conference*, (2013), paper PDP5A.6.
26. T. A. Eriksson, M. Sjödin, P. Andrekson, and M. Karlsson, "Experimental demonstration of 128-SP-QAM in uncompensated long-haul transmission," in *Optical Fiber Communication Conference/National Fiber Optic Engineers Conference*, (2013), paper OTu3B.2.
27. J. Renaudier, O. Bertran-Pardo, A. Ghazisaeidi, P. Tran, H. Mardoyan, P. Brindel, A. Voicila, G. Charlet, and S. Bigo, "Experimental transmission of Nyquist pulse shaped 4-D coded modulation using dual polarization 16QAM set-partitioning schemes at 28 Gbaud," in *Optical Fiber Communication Conference/National Fiber Optic Engineers Conference*, (2013), paper OTu3B.1.
28. P. Johannisson, M. Sjödin, M. Karlsson, H. Wymeersch, E. Agrell, and P. Andrekson, "Modified constant modulus algorithm for polarization-switched QPSK," Opt. Express **19**, 7734–7741 (2011).
29. S. J. Savory, "Digital coherent optical receivers: algorithms and subsystems," IEEE J. Sel. Top. Quantum Electron. **16**, 1164–1179 (2010).
30. T. Pfau, S. Hoffmann, and R. Noé, "Hardware-efficient coherent digital receiver concept with feedforward carrier recovery for *M*-QAM constellations," J. Lightwave Technol. **27**, 989–999 (2009).
31. J. Conway and N. Sloane, "Fast quantizing and decoding and algorithms for lattice quantizers and codes," IEEE Trans. Inf. Theory **28**, 227–232 (1982).
32. F. Pittalà, F. Hauske, Y. Ye, I. Tafur Monroy, and J. Nossek, "Training-based channel estimation for signal equalization and OPM in 16-QAM optical transmission systems," *European Conference and Exhibition on Optical Communication*, (2012), paper P3.16.
33. B. Krongold, T. Pfau, N. Kaneda, and S. Lee, "Comparison between PS-QPSK and PDM-QPSK with equal rate and bandwidth," IEEE Photon. Technol. Lett. **24**, 203–205 (2012).
34. T. Pfau, B. Krongold, S. Lee and N. Kaneda, "Comparison of bandwidth expansion methods for optical transmission systems," in *Opto-Electronics and Communications Conference*, (2012), paper 5B4-1.

#192613 - $15.00 USD Received 19 Jun 2013; revised 29 Jul 2013; accepted 29 Jul 2013; published 7 Aug 2013

1. Introduction

The optical coherent receiver has enabled fiber optical communication systems using modulation formats which take advantage of both quadratures as well as the two polarization states of the optical field and we have seen a remarkable amount of research on high-speed optical links utilizing such modulation formats in combination with polarization multiplexing. The two modulation formats that have been most studied in coherent optical communication systems are polarization multiplexed (PM) quadrature phase shift keying (QPSK) and polarization multiplexed rectangular 16-ary quadrature amplitude modulation (PM-16QAM). The development of systems utilizing these formats has been possible much due to the use of digital signal processing (DSP) which has been enabled by the increased speed of electronics of the last decades. The use of phase-tracking, polarization demultiplexing and adaptive equalization in the DSP has made transmission of these two formats and a plethora of other modulation formats possible. PM-QPSK is by far the most studied modulation format in coherent optical links and has been investigated using off-line processing in countless experiments and also implemented using real-time DSP [1,2]. PM-16QAM enables higher spectral efficiency at a cost of a reduced transmission reach and has been extensively studied recently [3, 4].

In 2009, the publications by Bülow [5] as well as Agrell and Karlsson [6, 7] triggered a new research trend on power efficient modulation formats. These are often called 4-dimensional (4D) modulation formats due to the fact that they are optimized in the four dimensions spanned by the two quadratures and the two polarization states of an optical field to achieve a large minimum Euclidean distance between the symbols. In contrast, conventional polarization multiplexed formats, such as PM-QPSK and PM-16QAM, are only optimized in the two dimensions spanned by the quadratures of each field component and the two polarization states are seen as independent channels for these 2-dimensional (2D) formats. Using sphere-packing in four dimensions, Agrell and Karlsson identified polarization-switched QPSK (PS-QPSK) which has an asymptotic sensitivity gain of 1.76 dB over PM-QPSK and is the most power efficient modulation format in four dimensions [6, 7]. The same format can also be realized using Ungerboeck's set-partitioning scheme on PM-QPSK [8]. PS-QPSK has received a lot of attention and has been experimentally studied in for instance [9–11]. Bülow introduced polarization-QAM (POL-QAM) where QPSK is modulated on six polarization states without any loss in sensitivity [5]. POL-QAM was experimentally demonstrated in [12, 13]. Agrell and Karlsson also proposed a 16 level 4D-format, called $C_{4,16}$ or OPT16, with the same spectral efficiency (SE) as PM-QPSK but with a 1.1 dB better asymptotic power efficiency [6, 14]. This format has been experimentally studied in [13]. Even more sensitive modulation formats can be achieved by increasing the dimensionality by for instance pulse-position modulation (PPM) [15, 16] or a combination of frequency-shift keying (FSK) and PPM [17]. However, going to higher order PPM decreases the SE significantly [15].

Modulation formats with high SE can be achieved by an increase in the number of signaling levels by going, e.g., to 512-QAM [18] or 1024-QAM [19]. However, in these cases the power efficiency is instead decreased. Coelho and Hanik [20] introduced 4D modulation formats that apply Ungerboeck's set-partitioning (SP) scheme to PM-16QAM [8]. These are called 32-level set-partitioning QAM (32-SP-QAM) and 128-level set-partitioning QAM (128-SP-QAM) and this concept can also be extended to using SP on higher order QAM formats [21]. The SP family of formats can achieve significant gain in power efficiency compared to conventional polarization multiplexed QAM formats while the reduction in SE is modest. Furthermore, since the SP-formats are based on rectangular-QAM formats, they can be implemented with similar hardware. 128-SP-QAM and 32-SP-QAM has been investigated in numerical simulations in [22] were the performance is compared to PM-QPSK and PM-8QAM with forward error-correction coding. A more extensive numerical study on 128-SP-QAM was done in [23] were it was shown

#192613 - $15.00 USD Received 19 Jun 2013; revised 29 Jul 2013; accepted 29 Jul 2013; published 7 Aug 2013

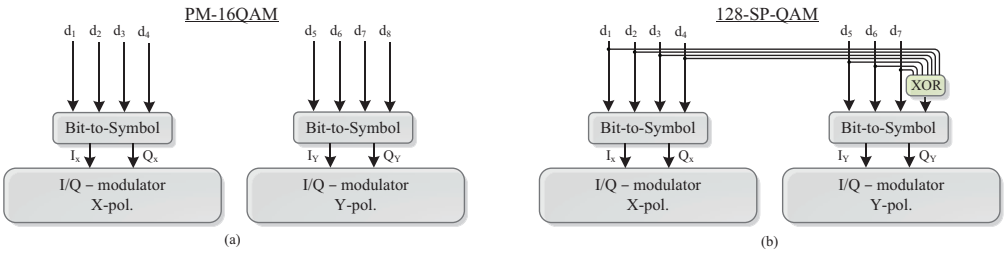

Fig. 1. Concept for (a) generating PM-16QAM and (b) generating 128-SP-QAM

that 128-SP-QAM is capable of achieving more than 40 % increase in transmission reach over PM-16QAM at the same bit rate for both single channel and WDM cases. A combination of PM-16QAM and 128-SP-QAM has been used to set a capacity-distance record [24] and a SE-distance record [25]. 128-SP-QAM has been experimentally investigated and its performance has been compared to PM-16QAM at the same symbol rate in single channel experiments [26]. 128-SP-QAM has also been experimentally investigated and compared to PM-16QAM as well as to 32-SP-QAM in a WDM setup using Nyquist pulse shaping, also at the same symbol rate for the formats [27]. In these two experimental investigations it was shown that 128-SP-QAM has a significant advantage in transmission reach compared to PM-16QAM at the same symbol rate.

In this paper, we present an experimental study of 128-SP-QAM in long-haul transmission and compare the results to PM-16QAM. We compare the formats both in single channel and in WDM transmission at a bit rate per channel of 80 Gbit/s and a channel spacing of 25 GHz. We also compare the formats at the same symbol rate (10.5 Gbaud) with the same channel spacing. This can also be of practical interest as a fall-back solution in degrading PM-16QAM links. We show that 128-SP-QAM can achieve a 1.9 dB increased back-to-back (B2B) sensitivity over PM-16QAM for the same bit rate and 2.9 dB for the same symbol rate. Compared at the same bit rate, we are able to transmit 128-SP-QAM 51 % longer than PM-16QAM in a single channel case and 54 % for WDM. For the same symbol rate the corresponding numbers are 55 % for single channel and 69 % for WDM transmission.

2. Description of 128-SP-QAM

128-SP-QAM is realized using set-partitioning on the Gray-coded PM-16QAM symbol alphabet which gives two subsets with even and odd parity, respectively. One of these subsets are chosen to get 128-SP-QAM. This means that 128-SP-QAM carries 7 bits per symbol compared to the 8 bits per symbol of PM-16QAM and that the minimum Euclidian distance between the constellation points is increased by $\sqrt{2}$ compared to PM-16QAM. It should be noted that it is also possible to perform a bit-to-symbol mapping with differential coding for 128-SP-QAM which was shown in [23].

The asymptotic power efficiency, γ, for any M-ary modulation format is given by

$$\gamma = \frac{d_{min}^2 \log_2 M}{4E_s}, \tag{1}$$

where d_{min} is the minimum Euclidean distance between the constellation points and E_s is the average symbol energy [7]. The factor $1/4$ normalizes the power efficiency to 0 dB for BPSK and QPSK. The 4D PM-16QAM constellation has $M = 256$ points, $d_{min} = 2$ and $E_s = 20$, giving $\gamma = -3.98$ dB. For 128-SP-QAM, $M = 128$, $d_{min} = 2\sqrt{2}$ and $E_s = 20$, resulting in $\gamma = -1.55$ dB.

#192613 - $15.00 USD Received 19 Jun 2013; revised 29 Jul 2013; accepted 29 Jul 2013; published 7 Aug 2013

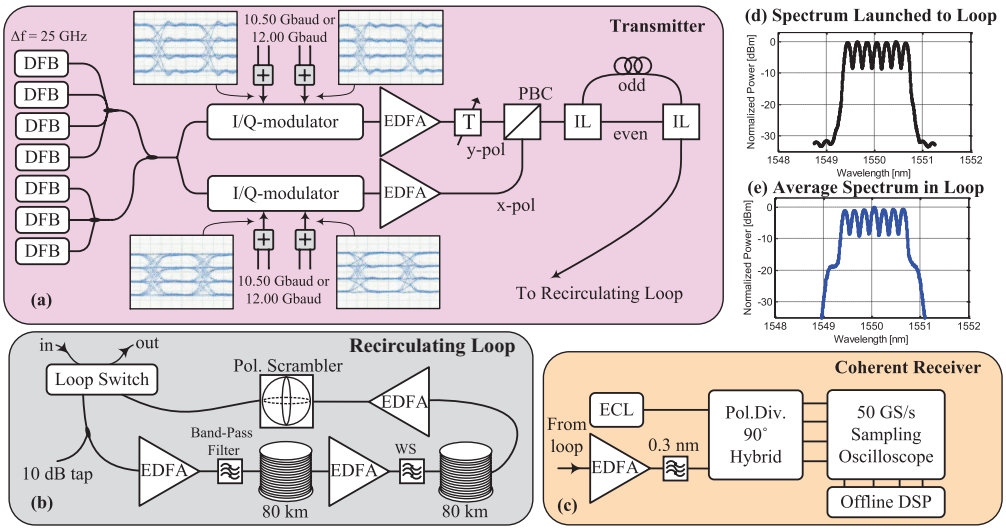

Fig. 2. Experimental setup showing: (a) The transmitter for both PM-16QAM and 128-SP-QAM including electrical eye diagrams of the four 10.5 Gbaud 4PAM driving signals to the I/Q-modulators. (b) The recirculating loop consisting of two spans of 80 km SMF. The band-pass filter is used to suppress out of band ASE noise and the waveshaper (WS) is used both as a band-pass filter and as a gain flattening filter. (c) The coherent receiver. (d) The spectrum launched to the loop in the case of WDM transmission (e) The average spectrum in the loop using the waveshaper as gain flattening filter.

The spectral efficiency SE per polarization for any N-dimensional modulation format is

$$SE = \frac{\log_2 M}{N/2}, \tag{2}$$

which gives PM-16QAM a SE of 4 bit/symbol/pol and 128-SP-QAM 3.5 bit/symbol/pol [21]. Thus, the symbol rate of 128-SP-QAM has to be increased by $1/7$ for the two formats to have the same bit rate.

2.1. Generation of 128-SP-QAM

Set-partitioning schemes can be implemented experimentally with minor addition in complexity to a typical polarization diverse QAM transmitter. The concept for a typical PM-16QAM transmitter is shown in Fig. 1a, where eight binary sequences are combined into 4-level signals to modulate 16QAM on the two polarization states. For 128-SP-QAM a constant parity is needed which can be achieved by encoding one of the bit sequences as an XOR-operation on the other seven as seen in Fig. 1b. This means that the transmitter architecture for PM-16QAM can be used for generating 128-SP-QAM with only minor additions to the complexity. The same concept can be used for 32-SP-QAM and 64-SP-QAM, only using more XOR-gates [22].

3. Experimental setup

The experimental setup for both PM-16QAM and 128-SP-QAM is shown in Fig. 2a. As light sources we use seven distributed feedback lasers (DFB), with ∼100 kHz linewidth, configured to a 25 GHz grid. For single channel experiments, only the center DFB is used. The transmitter is based on one I/Q-modulator per polarization. The I/Q-modulators are driven by four 4-ary

#192613 - $15.00 USD Received 19 Jun 2013; revised 29 Jul 2013; accepted 29 Jul 2013; published 7 Aug 2013

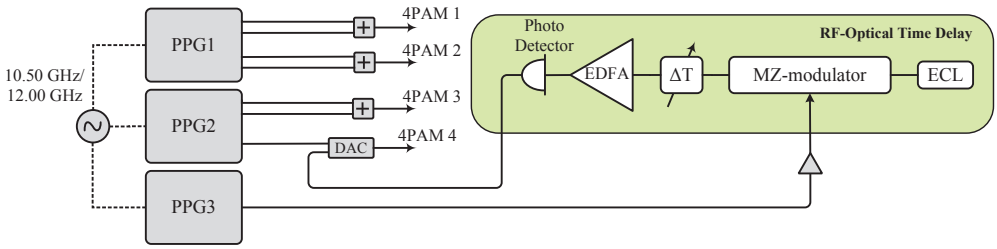

Fig. 3. Experimental setup for generation of the four 4-level signals needed to generate 128-SP-QAM and PM-16QAM. The RF-Optical delayline used to synchronize the patterns for 128-SP-QAM is also shown. The same setup is used for both PM-16QAM and 128-SP-QAM.

pulse amplitude modulation (4PAM) signals generated using three different pulse pattern generators (PPG) driven at 10.5 GHz or 12 GHz as shown in Fig. 3. The binary signals are pseudo random binary sequences (PRBS) with a length of $2^{15} - 1$. To generate 128-SP-QAM, the set-partitioning is achieved by programming one bit sequence as an XOR-operation on the other seven, as explained in section 2.1.

The start of the patterns from the three different PPGs could not be synchronized electronically so when a pattern was loaded in PPG3, the reference was lost to PPG1 and PPG2. A variable delay of several thousands of bits had to be used for the set-partitioning pattern from PPG3 and therefore the RF-optical delayline shown in Fig. 3 had to be implemented. The bit sequence from PPG3 is modulated onto an optical carrier using a Mach-Zehnder modulator (MZM) and an external cavity laser (ECL) as light source. The sequence can then be delayed in the optical domain, using fibers with different lengths, before being detected by a photo-detector and sent to a 3-bit digital-to-analogue converter (DAC) together with one pattern from PPG2.The DAC samples the input signals at the clock rate and the two binary signals are actively added with different weights to create a 4PAM signal. The DAC thus cleans up the signal after the photo-detector and does not suffer from the inherent loss of the passive combiner which we used in [26]. The DAC also made optimization of the constellations much easier and the noise characteristics of the produced 4PAM signal are similar to that of the other three 4PAM signals which are generated using passive power-combiners. For PM-16QAM the same setup is used but with a standard PRBS pattern from PPG3 instead of the set-partitioning pattern.

As seen in the electrical eye diagrams in Fig. 2a, the outputs from the different PPGs and the DAC have slightly different shapes creating 4PAM signals with slightly varying overshoot and rise-times. However, we observe no noticeable difference in terms of bit-error rate (BER) for the different signals after detection. The optical signals in the two polarization paths are amplified using erbium-doped fiber amplifiers (EDFA) before combined with orthogonal polarizations using a polarization beam combiner (PBC). An optical delayline is used in one polarization arm to align the symbols in time. After the PBC, the even and odd channels are split using an optical interleaver (IL) with 25 GHz channel spacing and decorrelated using $\sim$2 meters of fiber for the odd channels before combined using a second IL.

The signals can then be propagated through a recirculating loop. The power of the seven launched channels are adjusted to be within $\pm$0.5 dB relative to each other by changing the output power of the lasers and the launched WDM spectrum is shown in Fig. 2d. The loop consists of two spans of 80 km standard single mode fiber (SMF) with 17 dB loss each. After each span an EDFA with $\sim$5 dB noise figure compensates for the loss and the first span is preceded by a variable optical bandpass filter to suppress out-of-band amplified spontaneous emission noise (ASE). The second span is preceded by a waveshaper that acts both as a variable

#192613 - $15.00 USD Received 19 Jun 2013; revised 29 Jul 2013; accepted 29 Jul 2013; published 7 Aug 2013

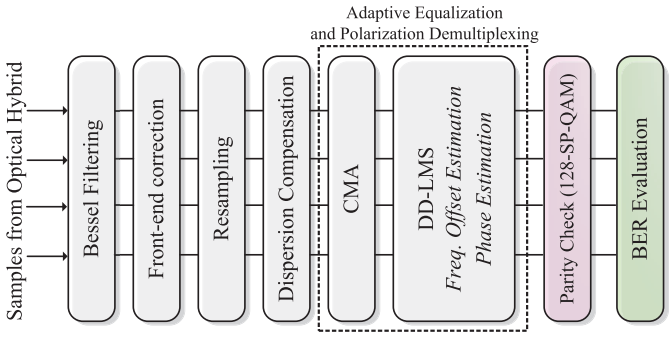

Fig. 4. Block-scheme of the digital signal processing flow for both 128-SP-QAM and PM-16QAM. For 128-SP-QAM a parity-check is performed and if the parity is incorrect, the most uncertain bit is inverted before the BER is evaluated [31].

optical bandpass filter and as a gain-flattening filter. A 10 dB tap is placed in the loop and the average power per channel over all roundtrips is measured with an optical spectrum analyzer (OSA) and the different channels are attenuated using the waveshaper to achieve a flatness of ± 1 dB. The average spectrum in the loop with gain flattening is shown in Fig. 2e. The bandwidth of the bandpass filter and the waveshaper is 1.5 nm for single channel experiments and 2.0 nm for the WDM experiments. A polarization scrambler that is synchronized to the roundtrip-time of the loop is used to avoid any unrealistic accumulation of polarization effects. Moreover, a third EDFA is used to compensate for the loss of the polarization scrambler and the loop-switching components.

The signals are detected using a polarization diverse 90° optical hybrid with integrated balanced detectors and amplifiers. A $\sim$300 kHz linewidth ECL is used as LO. The received signals are amplified by an EDFA followed by a 0.3 nm optical bandpass filter to suppress both ASE noise and the neighboring channels. The electrical signals from the hybrid are sampled using a 50 GSample/s real-time sampling oscilloscope with 16 GHz analogue bandwidth and the sampled data is processed offline.

4. Digital signal processing and decoding

The same DSP algorithms that are generally used for PM-16QAM can be used for 128-SP-QAM, which we confirm with experimental data in this paper and which was also found in the numerical simulations in [23]. As discussed in [23] this is not obvious, if we compare to PS-QPSK, which is a set-partitioned subset of PM-QPSK and for which it is not possible to perform polarization demultiplexing using the conventional constant modulus algorithm (CMA) [28]. The DSP components for both 128-SP-QAM and PM-16QAM are shown in Fig. 4. The DSP starts with a low-pass filtering using a 5th order Bessel filter with a bandwidth of 70 % of the symbol rate followed by optical front-end compensation with DC-offset estimation, I/Q-angle imperfection compensation based on Gram-Schmidt orthogonalization [29] and I/Q-amplitude imbalance compensation. The signals are then re-sampled to 2 samples per symbol and to compensate for the accumulated chromatic dispersion, a time-domain static finite impulse response (FIR) filter is used as described in [29] and references therein. To achieve polarization demultiplexing and linear equalization four 21-tap T/2 butterfly FIR filters are used. The tap coefficients are updated using first CMA [29] for pre-convergence followed by the decision-directed least-mean square (DD-LMS) algorithm for final adaptation. The fast Fourier transform-based (FFT) frequency offset estimation as well as the carrier phase estimation based on the blind phase search method [30] using 64 test-phases and a block length of 110 samples using 2 sam-

#192613 - $15.00 USD Received 19 Jun 2013; revised 29 Jul 2013; accepted 29 Jul 2013; published 7 Aug 2013

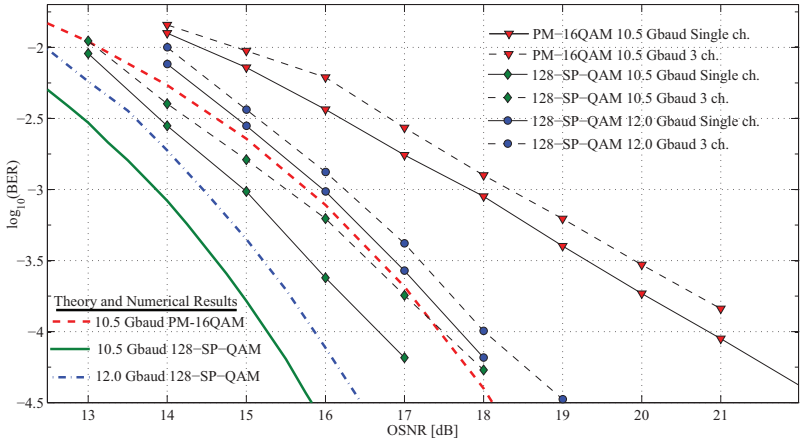

Fig. 5. Measured back to back performance showing BER as a function of OSNR for 10.5 Gbaud PM-16QAM (red triangles), 10.5 Gbaud 128-SP-QAM (green diamonds) and 12.0 Gbaud 128-SP-QAM (blue circles). Solid lines show single channel results and dashed lines show results where optical interleavers and two neighboring channels were present. The numerical results for 128-SP-QAM are achieved by Monte Carlo simulations with AWGN as the only impairment.

ple/symbol, are performed within the DD-LMS loop.

For the Gray-coded PM-16QAM, rectangular decision regions are used for symbol detection. To decode 128-SP-QAM the method described in [31] is used were the signal in the two polarizations first are independently decoded as Gray-coded 16QAM. If a detected 4-dimensional symbol has incorrect parity, the symbol is moved over its closest decision threshold which inverts the most uncertain bit. The parity bit is then discarded before the BER is evaluated.

It should be noted that both PM-16QAM and 128-SP-QAM have phase and polarization ambiguities due to the unknown absolute phase and polarization state of the received signal. The problem with phase ambiguities can be avoided using differential coding of the bits [23]. Another solution is to use training sequences to resolve the phase and polarization ambiguities as for instance in [32] or shown for a 4D-modulation format in [12]. In this work however, the ambiguity problems were resolved by using the knowledge of the transmitted PRBS sequences.

5. Results and discussion

The B2B performance for 10.5 Gbaud PM-16QAM, 10.5 Gbaud and 12 Gbaud 128-SP-QAM as well as theoretical and numerical results are shown in Fig. 5. The numerical results for 128-SP-QAM are found using Monte Carlo simulations with one sample per symbol and additive white Gaussian noise (AWGN) as the only impairment. We define implementation penalty as the difference in the optical signal to noise ratio (OSNR) required to achieve BER = 10^{-3} and the theoretically or numerically predicted OSNR requirement for the same BER. For PM-16QAM, the implementation penalty was measured to 2.1 dB and for 128-SP-QAM at 10.5 Gbaud and 12 Gbaud it was found to be 1.1 dB and 1.5 dB respectively. The higher implementation penalty for PM-16QAM can be attributed to the fact that PM-16QAM has a smaller minimum Euclidian distance between the symbols and thus it is more sensitive to non-idealities in the driving signals. Compared to the B2B results we saw in [26], the changes in the transmitter side improved the performance of 128-SP-QAM by 0.3 dB while for PM-16QAM it is approximately the same. At BER = 10^{-3}, 128-SP-QAM has 2.9 dB better sensitivity than PM-

#192613 - $15.00 USD Received 19 Jun 2013; revised 29 Jul 2013; accepted 29 Jul 2013; published 7 Aug 2013

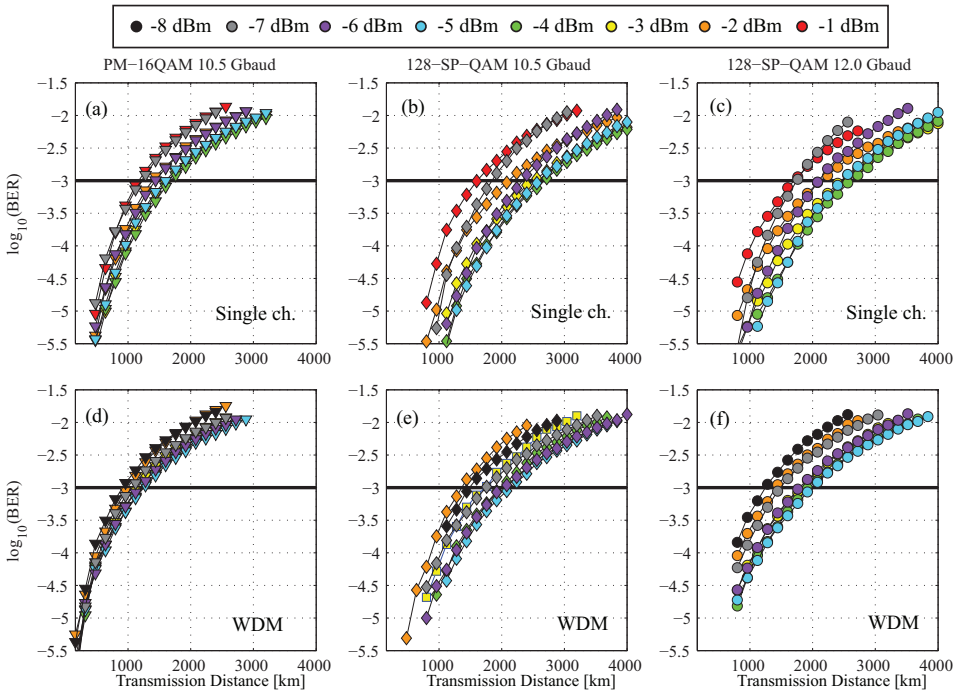

Fig. 6. Transmission results for different launch powers showing (a) single channel transmission of PM-16QAM at 10.5 Gbaud, (b) single channel transmission of 128-SP-QAM at 10.5 Gbaud, (c) single channel transmission of 128-SP-QAM at 12.0 Gbaud, (d) WDM transmission of PM-16QAM, (e) WDM transmission of 128-SP-QAM at 10.5 Gbaud and (f) WDM transmission of 128-SP-QAM at 12.0 Gbaud.

16QAM for the same symbol rate and 1.9 dB better sensitivity at the same bit rate. We also investigated the linear crosstalk penalty and filtering penalties from the optical interleavers by measuring B2B performance with two neighboring channels of the center channel switched on. This penalty is found to be less then 0.5 dB for all formats.

The transmission results for 10.5 Gbaud PM-16QAM, 10.5 Gbaud 128-SP-QAM and 12 Gbaud 128-SP-QAM for both single channel and WDM transmission and for varying launch powers are shown in Fig. 6. Single channel PM-16QAM is shown in Fig. 6a and WDM transmission is shown in Fig. 6d. Further, single channel and WDM transmission of 128-SP-QAM at the same symbol rate (10.5 Gbaud) as PM-16QAM is shown in Fig. 6b and Fig. 6e respectively. Finally, single channel and WDM transmission of 128-SP-QAM where the symbol rate has been increased to 12 Gbaud to achieve the same bit rate as PM-16QAM is shown in Fig. 6c and Fig. 6f respectively. The optimal launch power is evaluated at BER = 10^{-3} and is found to be -4 dBm for the single channel transmission of 10.5 Gbaud PM-16QAM, 10.5 Gbaud 128-SP-QAM and 12 Gbaud 128-SP-QAM. For WDM transmission, the optimal launch power per channel is -5 dBm for all three cases. It should be noted that for some cases the difference in transmission reach of the optimal launch power and launch powers close to the optimal, yields very similar results at BER = 10^{-3}. For instance, Fig. 6e shows minor impairments when going from -5 dBm (optimal) to -4 dBm which is also true for Fig. 6d. We also observe that PM-16QAM is less sensitive to changes in launch power, although it should be noted that 128-SP-QAM is transmitted over longer distances and thus will accumulate more nonlinear distortion.

#192613 - $15.00 USD Received 19 Jun 2013; revised 29 Jul 2013; accepted 29 Jul 2013; published 7 Aug 2013

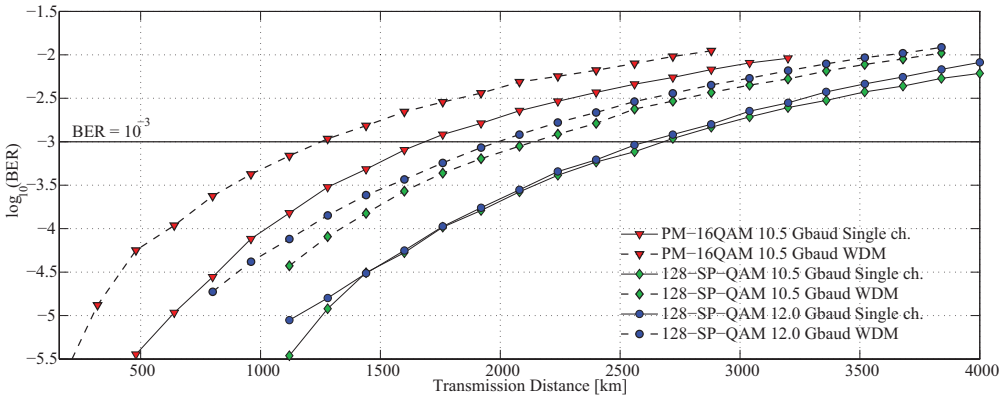

Fig. 7. Transmission results for the optimized launch power at BER = 10^{-3} for 10.5 Gbaud PM-16QAM (red triangles), 10.5 Gbaud 128-SP-QAM (green diamonds) and 12.0 Gbaud 128-SP-QAM (blue circles). Solid lines show single channel and dashed lines WDM transmission.

5.1. Single channel transmission

In Fig. 7, the transmission results for all cases using the optimal launch power for longest transmission reach at BER = 10^{-3} are shown. The optimal launch power for each case is maintained for all transmission distances in Fig. 7. In this and the next section, we compare all formats at BER = 10^{-3}. If we first compare the two formats using the same symbol rate of 10.5 Gbaud we see that for single channel transmission (shown as solid lines in Fig. 7), PM-16QAM can be transmitted up to 1730 km and 128-SP-QAM up to 2680 km. This corresponds to an increased transmission reach of 55 % and is in good agreement with what was observed in [26]. If we increase the symbol rate of 128-SP-QAM to 12 Gbaud the transmission reach is 2610 km. This corresponds to 51 % longer transmission reach over PM-16QAM which is still a substantial improvement.

5.2. WDM transmission

WDM transmission for the three cases are shown as dashed lines in Fig. 7. We first observe a penalty in the transmission reach for going from single channel transmission to WDM of 34 % for 10.5 Gbaud PM-16QAM, 25 % for 10.5 Gbaud 128-SP-QAM and 31 % for 12 Gbaud 128-SP-QAM. PM-16QAM can be transmitted up to 1300 km while 10.5 Gbaud 128-SP-QAM can be transmitted up to 2140 km which is an increase of 69 %. 12 Gbaud 128-SP-QAM can be transmitted up to 1990 km which corresponds to an increase of 54 % over PM-16QAM. It should be noted that this increase is roughly the same as the increase seen for 128-SP-QAM over PM-16QAM at the same bit rate in single channel transmission. However, for 128-SP-QAM at 10.5 Gbaud, we see 10 % additional increase compared to that of single channel transmission. We conclude that PM-16QAM is more affected by WDM transmission impairments compared to 128-SP-QAM. However, increasing the symbol rate of 128-SP-QAM to 12 Gbaud brings the penalty compared to single channel case closer to that of PM-16QAM. This is likely to be due to extra penalty from filtering effects in the optical interleavers and also less tolerance to crosstalk. However, the observed increase of 54 % in WDM transmission distance for 128-SP-QAM compared to PM-16QAM at the same bit rate is still a substantial advantage. These results are in good agreement with the numerical simulations in [23] where a 40-50 % increase in transmission reach is reported for both the single channel and the WDM case at the same bit

#192613 - $15.00 USD Received 19 Jun 2013; revised 29 Jul 2013; accepted 29 Jul 2013; published 7 Aug 2013

rate. The 69 % increased reach when comparing the two formats at at the same symbol rate in WDM transmission is slightly lower than what is reported in the experiment in [27]. However, in [27] the symbol rate is 28 Gbaud with a WDM spacing of 33 GHz which together with the fact that Nyquist shaped pulses are used makes the systems in [27] and in this paper somewhat hard to compare.

5.3. Forward error correction coding

In [33, 34], PS-QPSK and PM-QPSK are compared at the same bit rate when forward error correcting codes (FEC) with different rates are applied to the two formats, and it is argued that PM-QPSK with a larger overhead code could possibly outperform uncoded PS-QPSK. A similar comparison would likely show that 16QAM would outperform both PM-QPSK and 128-SP-QAM, since the extra bit(s) could be used for FEC overhead. In this publication however, we argue that for a flexible system with the possibility to use both 128-SP-QAM and PM-16QAM it is anticipated that the same FEC will be used for both formats as a separate subsystem. Also, using a different, lower rate, code for PM-16QAM leads to a more complex system, especially in terms of framing and buffering. To compare the two formats in a fair way with coding, codes with good performance, similar complexity but with different rates should be used, which is not trivial and beyond the scope of this work.

Comparing the two formats and assuming that the same code will be used for both formats, we expect to see a similar gain in transmission reach for 128-SP-QAM over PM-16QAM also after FEC decoding. It should be noted though that when comparing 128-SP-QAM to higher order QAM such as PM-16QAM with larger overhead it likely exist a code that can outperform 128-SP-QAM after decoding, at the price of higher complexity.

Finally, as noted by an anonymous referee, the use of soft FEC has the potential of aiding the parity-demodulation of 128-SP-QAM in a joint demodulation and decoding stage. This possibility, while interesting, requires substantial work and has to be deferred to future studies.

6. Conclusions

We have experimentally demonstrated 128-SP-QAM in single channel and WDM transmission and compared the results to PM-16QAM both at the same symbol rate and at the same bit rate. We have verified that 128-SP-QAM can achieve a higher sensitivity compared to PM-16QAM and shown a 2.9 dB increased sensitivity at a BER = 10^{-3} at the same symbol rate and 1.9 dB at the same bit rate. In single channel transmission we have shown that 128-SP-QAM can achieve 51 % longer reach compared to PM-16QAM at the same bit rate and 55 % at the same symbol rate. In WDM transmission we have shown 54 % increased transmission reach for 128-SP-QAM over PM-16QAM at the same bit rate and 69 % at the same symbol rate.

Acknowledgments

The authors would like to acknowledge the financial support from the Swedish Research Council (VR).

#192613 - $15.00 USD Received 19 Jun 2013; revised 29 Jul 2013; accepted 29 Jul 2013; published 7 Aug 2013